

# New, Generally Applicable Metrics for RAIM/AAIM Integrity Monitoring

P.B. Ober

*Delft University of Technology  
Telecommunications and Traffic Control Systems Group  
Mekelweg 4, 2628 CD Delft, The Netherlands*

## BIOGRAPHY

Bastiaan Ober has 3 years of experience in the field of radio navigation. He received his M.Sc. in Electrical Engineering from Delft University of Technology in 1993. His thesis treats the fast computation of integer ambiguities for carrier phase GPS with the basis reduction method. Further areas of experience include the influence of multipath on GPS positioning, carrier phase differential GPS, and integrity of GPS and integrated navigation systems. He is currently working as a Ph.D. student at Delft University of Technology, The Netherlands, doing research on the design of optimal integrity monitoring algorithms for integrated navigation systems.

## ABSTRACT

In this paper, we will develop a new integrity metric for navigation systems, that we will call the Bias Integrity Threat (BIT), and a derivative of it, the Maximum Undetectable Position Bias (MUPB). Integrity metrics are used to indicate whether a navigation system has sufficient error detection power. As we will see, integrity depends on both measurement geometry and measurement quality, that is, the standard deviation of the

measurement noise. Existing metrics like the  $\delta H_{\max}$  [Sturza90] and the ARP [Brown92b] have two serious limitations: they can not be applied straightforwardly for measurements of different standard deviations, or for multiple failures. Also, they can not be used in a Kalman filter environment. Because these metrics do not take the noise level into account, the values of  $\delta H_{\max}$  and the ARP are relative, rather than absolute measures of integrity, which makes it hard to interpret their values. We will illustrate this in section 7.

The BIT and MUPB do not possess any of these disadvantages: they can be used with general measurement covariance matrices, and are well defined for the assumption of multiple failures. They are therefore applicable in a wide range of applications, including Kalman filter environments. Furthermore, their values are absolute and thus more suitable for comparing the integrity of different navigation systems than the traditional integrity measures. Their computational needs are modest, allowing their use in real time applications.

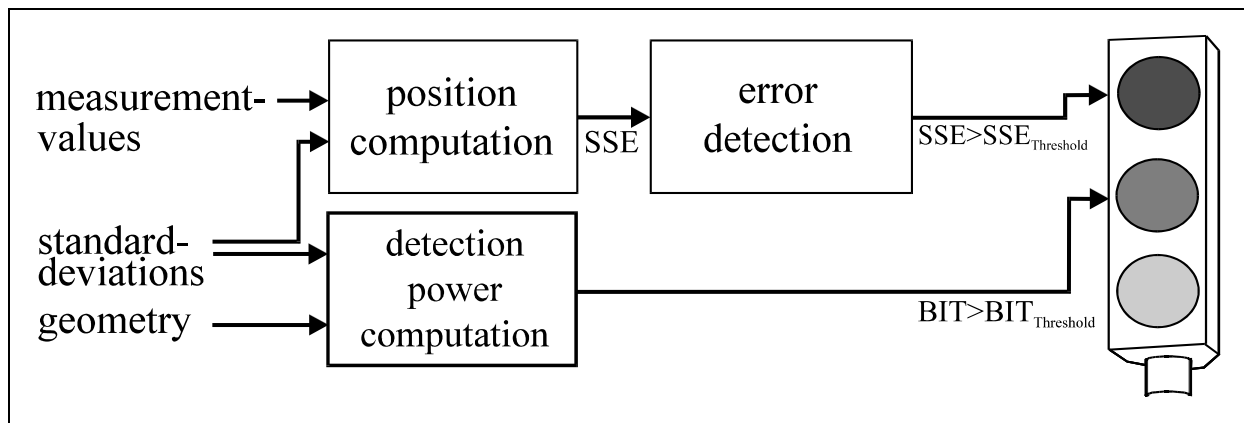


Figure 1. An Integrity Monitor with its input and output signals

## 1. Introduction

Integrity is the ability of a navigation system to provide timely warnings when the user should not use the system for navigation. This means that the user needs to be warned when the system can not guarantee that it is working within the required specifications. In this paper, we will focus on integrity monitoring methods that do not use external systems. Two techniques can be distinguished. Receiver Autonomous Integrity Monitoring (RAIM) only uses the signals that are provided by GPS receivers, Aircraft Autonomous Integrity Monitoring (AAIM) uses information from other sensors as well. Under the assumption that all sensors are fully integrated and used in the position solution, there is no fundamental difference between RAIM and AAIM, and we will not differentiate between the two.

An integrity monitoring system must consist of two parts (see also figure 1):

### 1. An Error Detector

The error detector will warn the user in case the system contains errors and should not be used. It uses redundancy in the signals to compute a test statistic (usually the residual of the position computation) that becomes larger when the mutual consistency of the signals becomes lower. If the test statistic surpasses a certain threshold, an error is detected and the user is shown a red light.

### 2. An Error Detectability Monitor

The second part of the system is the ‘error detectability monitor’, that computes whether enough redundancy is present to be able to detect errors with sufficient reliability. If this is not the case, the system lacks detection power, and the user is shown a yellow light. This part is the actual integrity monitor, but because the error detectability it computes is only meaningful in combination with a certain error detector, the latter is usually assumed to be an integral part of the monitor as well. As we will see, the error detectability is a function of both the measurement geometry and standard deviation.

After the introduction of the system model in section 2, we will first describe a common error detection scheme in section 3. Then, we will discuss two currently existing error detectability (integrity) metrics called  $\delta H_{\max}$  and ARP in section 4 and 5. We show the disadvantages of these metrics in section 6. In section 7 we introduce a new metric called Bias Integrity Threat (BIT), that is also well defined for multiple measurement biases (section 8). A derived integrity metric, the Maximum Undetectable Position Bias (MUPB), is presented in section 9. Section 10 shows how the BIT and MUPB can be applied in a

Kalman filter environment. The appendix will illustrate how to compute the BIT in a multiple bias scenario.

## 2. The system model

We will assume that the relation between the measurements that the navigation system provides, and the actual position of the user, is given by an overdetermined linear regression model:

$$\bar{z} = H \cdot \bar{x} + \bar{v} \quad (2.1)$$

in which:

$\bar{z}$  :  $n$ -vector of measurements

$H$  :  $n \times m$  observation matrix

$\bar{x}$  :  $m$ -vector of unknowns (position, clock bias)

$\bar{v}$  :  $n$ -vector with independent noise and biases in the measurements, normally distributed  $\sim N(\bar{\mu}_v, R_v)$

with  $n > m$ .

In case of no error, the noise is assumed to be unbiased (that is, zero mean), but when errors are present, the mean will deviate from zero. We want to detect such deviations, and can formulate the error detection problem as the following hypotheses testing problem on the mean of the noise (that we will call *bias* from now on):

$$\begin{aligned} H_0 \text{ (no error): } & \bar{\mu}_v = \bar{0} \\ H_1 \text{ (error): } & \bar{\mu}_v \neq \bar{0} \end{aligned} \quad (2.2)$$

To test between these hypotheses, we have to estimate the bias  $\bar{\mu}_v$ . We will discuss this in the next section.

## 3. Position and bias estimation

It is well known [Rao95] that when the noise is normally distributed, the best (minimum covariance) linear estimation of the position is given by a weighted least squares solution of (2.1):

$$\hat{\bar{x}}_{LS} = N\bar{z} \quad (3.1)$$

with

$$N = (H^T R_v^{-1} H)^{-1} H^T R_v^{-1} \quad (3.2)$$

This estimation is normally distributed:

$$\hat{\bar{x}}_{LS} \sim N(\bar{\mu}_{\hat{x}}, R_{\hat{x}}) \quad (3.3)$$

with mean and covariance

$$\tilde{\mu}_{\hat{x}} = \bar{x} + \Delta\hat{x}_{LS} \quad (3.4)$$

$$R_{\hat{x}} = (H^T R_v^{-1} H)^{-1} \quad (3.5)$$

where we have written the position error that is caused by the bias as

$$\Delta\hat{x}_{LS} = N\tilde{\mu}_v \quad (3.6)$$

The linear model (2.1) can be seen as a decomposition of the observation vector  $\vec{z}$  into a nonstochastic part  $H\bar{x}$  and a stochastic part  $\vec{v}$ . When we remove the estimated nonstochastic part, we obtain the best estimation of the noise as the least squares residual:

$$\hat{v}_{LS} = D\vec{z} \quad (3.7)$$

with

$$D = (I - H(H^T R_v^{-1} H)^{-1} H^T R_v^{-1}) = (I - HN) \quad (3.8)$$

The estimated noise is normally distributed

$$\hat{v}_{LS} \sim N(\tilde{\mu}_{\hat{v}}, R_{\hat{v}}) \quad (3.9)$$

with mean and covariance

$$\tilde{\mu}_{\hat{v}} = D\tilde{\mu}_v \quad (3.10)$$

$$R_{\hat{v}} = DR_v D^T \quad (3.11)$$

Note that both the position and the noise estimation are only unbiased when  $\tilde{\mu}_v = \vec{0}$ . Another important observation is that the matrix  $D$  has rank  $n-m$ . This means that  $\tilde{\mu}_{\hat{v}}$  can become zero when more than  $n-m$  elements of  $\tilde{\mu}_v$  are nonzero, that is, when more than  $n-m$  measurements are in error simultaneously. In that situation, the worst case error detectability drops to zero.

The estimation of the noise can be used to test between the two hypotheses of (2.2). Usually, the test is not done on the separate components of  $\hat{v}_{LS}$ , but on its total length, normalized by the noise covariance. The test statistic<sup>1</sup> becomes

<sup>1</sup> In RAIM literature, sometimes the RRP (Range Residual Parameter), [Parkinson88] [Brown96], is used. The RRP is monotonically related to the SSE and therefore has similar properties:

$$RRP = \sqrt{\frac{SSE}{n-m}}$$

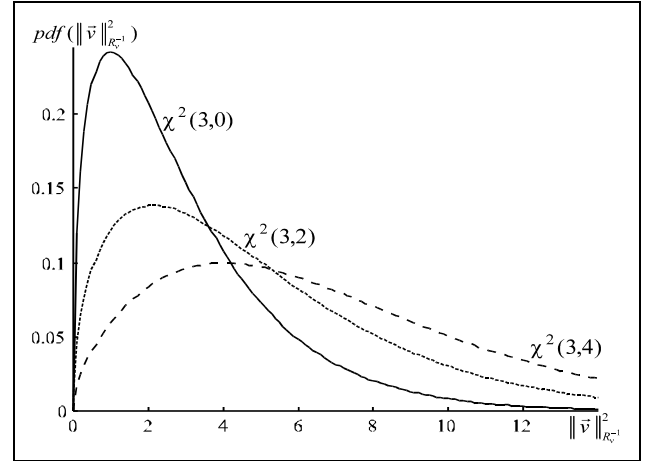


**Figure 2. Probability distribution function of central and noncentral chi-square distributions with 3 degrees of freedom**

$$SSE = \left\| \hat{v}_{LS} \right\|_{R_v^{-1}}^2 = \hat{v}_{LS}^T R_v^{-1} \hat{v}_{LS} \quad (3.12)$$

where SSE stands for “sum of squares of (range residual) errors”. The test statistic SSE has a noncentral chi-square distribution with  $n-m$  degrees of freedom and a noncentrality  $\lambda$ :

$$SSE \sim \chi^2(n-m, \lambda) \quad (3.13)$$

with

$$\lambda = \tilde{\mu}_v^T D^T R_v^{-1} D \tilde{\mu}_v = \tilde{\mu}_{\hat{v}}^T R_{\hat{v}}^{-1} \tilde{\mu}_{\hat{v}} \quad (3.14)$$

This means that the test between the ‘no error’ and ‘error’ hypotheses is equivalent to a test on the noncentrality parameter of the distribution of the SSE:

$$H_0 \text{ (no error): } \lambda = 0 \quad (3.15)$$

$$H_1 \text{ (error): } \lambda > 0$$

The test statistic has an expected value that grows linearly with the noncentrality parameter

$$E\{SSE\} = \lambda + n - m \quad (3.16)$$

and is therefore suitable to perform test (3.15). The final decision will be taken by putting a threshold on the SSE. If the threshold is exceeded, the ‘no error’ hypothesis is supposed to be too unlikely, and an error is detected:

$$H_0 \text{ (no error): } SSE \leq SSE_{threshold} \quad (3.17)$$

$$H_1 \text{ (error): } SSE > SSE_{threshold}$$

Figure 2 shows some noncentral chi-square distributions for 3 degrees of freedom and different values of  $\lambda$ . Indeed, we see that large values of the test statistic are very unlikely for the ‘errorfree’ distribution ( $\lambda=0$ ), and are therefore much likelier to be caused by biases ( $\lambda>0$ ) than by noise.

The noncentrality  $\lambda$  depends on the unknown size and direction of the bias, as well as on the known measurement geometry that is reflected in  $H$ . The more favorable the geometry, the larger  $\lambda$  will become for a certain bias, and the easier it will be to detect this bias.

#### 4. Error detectability: $\delta H_{\max}$ (integrity DOP)

In this section, we will discuss the integrity parameter known as  $\delta H_{\max}$  or integrity DOP (iDOP), that is a measure for the error detectability that a certain measurement configuration offers.

Suppose one measurement  $i$  contains a bias. If the remaining measurements show a weak geometry, they provide only inaccurate position information, making it hard to check the correctness of measurement  $i$ . Moreover, if measurement  $i$  is responsible for a good overall geometry, its bias will cause a position error that is relatively large compared to the obtained precision. An intuitive and often used measure of integrity can therefore be defined as the worst reduction in position precision, measured in DOP, caused by removing one measurement from the solution. This ‘integrity geometry’ or ‘integrity DOP’ is a worst case parameter that is defined as

$$iDOP = \max_i DOP_i^2 - DOP^2 \quad (4.1)$$

in which DOP is the ‘all in view’ dilution of precision:

$$DOP = \sqrt{\text{trace}(H^T H)^{-1}} \quad (4.2)$$

and  $DOP_i$  is the DOP of the solution in which measurement  $i$  has been omitted. The integrity DOP was introduced in [Brown90] and [Sturza90], where it was called  $\delta H_{\max}$ . We will continue to use the more descriptive term integrity DOP (iDOP), because it plays the same role in failure detection as the DOP does in the navigation problem. Because of the way it is defined, the integrity DOP is only meaningful:

- for independent measurements with identical noise variances
- for the linear regression model
- for the assumption of a single failure

In the next section we will discuss an equivalent description of the integrity DOP, that will help us to find a more generally applicable metric in section 7.

#### 5. Error detectability: the ARP

As we showed in section 3, a measurement bias will cause both a position estimation error and a larger test statistic. Its exact influence will depend on the measurement geometry. System integrity is guaranteed as long as the test statistic represents the position bias well. The minimum size of a bias that can be detected reliably is determined by the measurement noise, and it is important that the position error that this bias can cause remains within the specified requirements. It can be proven [Ober96], that the iDOP exactly equals the largest ratio of the position estimation bias (3.6) and the mean of the estimated noise (3.10) that a bias in a single measurement can cause. Note that this is only true in the case that all measurements are independent and have the same variance ( $R_i = \sigma^2 I$ ).

This means that the following definition of the iDOP is equivalent to (4.1):

$$iDOP = \max_i \frac{\|(H^T H)^{-1} H^T \bar{\mu}_v^{(i)}\|^2}{\|(I - H(H^T H)^{-1} H^T) \bar{\mu}_v^{(i)}\|^2} \quad (5.1)$$

Because we assume that only a single failure occurs (in the measurement indexed by  $i$ ), the bias vectors in (5.1) have the form

$$\bar{\mu}_v^{(i)} = [0 \dots 0 \quad \mu_i \quad 0 \dots 0]^T \quad (5.2)$$

When a certain threshold  $SSE_{\text{threshold}}$  for the test statistic is chosen, Brown [Brown92b] defines the following integrity metric:

$$ARP = \sqrt{iDOP \cdot SSE_{\text{threshold}}} \quad (5.3)$$

where ARP stands for Approximate Radial-error Protected. The ARP is an integrity metric that estimates the maximum position error that can remain undetected. It is based on the fact that, when there is no noise, the iDOP is exactly the ratio of position bias and test statistic for the worst measurement bias:

$$\text{no noise} \Rightarrow iDOP = \frac{\|\Delta \hat{x}_{LS}\|^2}{SSE} \quad (5.4)$$

Naturally, the largest position bias that remains undetected is obtained when we substitute

$SSE = SSE_{threshold}$ . Of course, measurement noise makes (5.4) too optimistic, and the actual position error that can be protected will be notably larger than the ARP of (5.3).

Although the two definitions of the iDOP (4.1) and (5.1) are mathematically identical, they offer two different intuitive explanations of the meaning of the value. As we will see (5.1) will prove to be more appropriate in the search for a generally usable integrity metric.

## 6. Disadvantages of geometric integrity metrics

As we have seen in the previous sections, the integrity metrics  $\delta H_{\max}$  (iDOP) and the ARP are purely geometric measures of integrity. We will show that this results in two disadvantages:

- They can not be used straightforwardly with measurements with different standard deviations
- Their values are not related to the actual noise level, but rather to a certain ‘standard noise level’. Therefore, they are not suitable to compare the integrity of different navigation systems and situations

Although this section will concentrate on the drawbacks of the iDOP, it should be clear that the ARP shares the same disadvantages, because it contains the iDOP in its definition<sup>2</sup>.

The iDOP assumes that the variance of all measurements is the same ( $R_v = \sigma^2 I$ ). If this is not the case, it can still be used after measurement scaling as was indicated in [Brown96]. Brown discusses the possibility of scaling individual measurements in such a way, that the scaled measurement residuals all have the same standard deviation again. His example covers the addition of GLONASS pseudorange measurements to the GPS pseudoranges:

If we denote the pseudoranges by  $PR_{GPS}$  and  $PR_{GLONASS}$ , and assume that

$$\sigma_{PR_{GLONASS}} = \frac{1}{2} \sigma_{PR_{GPS}} \quad (6.1)$$

the standard deviation of twice the GLONASS pseudorange equals the standard deviation of GPS:

$$\sigma_{2 \cdot PR_{GLONASS}} = 2 \cdot \sigma_{PR_{GLONASS}} = \sigma_{PR_{GPS}} \quad (6.2)$$

This means that when we multiply all rows of  $H$  that belong to GLONASS measurements by a factor 2, we can use the traditional integrity metrics again.

	iDOP	BIT
GLONASS scaled to GPS	52.8	1080
GPS scaled to GLONASS	3.3	1080
GPS only	2.5	2240
GLONASS only	2.5	560

**Table 1. Comparison between iDOP and BIT**

Unfortunately, the standard deviation to which the measurements are scaled will influence the values of iDOP, even though the integrity is not effected by such a scaling. The opposite can also happen: when we compare two situations with the same measurement geometry but different amounts of noise, the values of iDOP are the same, while the integrity will improve with a decrease of the noise.

We can illustrate this as follows. In the example provided above, we could also scale all GPS measurements to get GLONASS variances by multiplying all rows of  $H$  that belong to GPS measurements by 0.5. Table 1 shows what this means for the values of the iDOP (and of the BIT that we will introduce in the next section). The values of iDOP and BIT can not be compared easily, but the table is still useful in comparing the behavior of both integrity metrics in different navigation situations. We compute them for four different cases. The measurement geometry can be found in the appendix (see figure 5), and we used it with the following measurement sources:

1. Satellites 1 and 2 are GPS, satellites 3 and 4 are GLONASS. We scaled the GLONASS variances to GPS variances
2. idem, but this time we scaled the GPS variances to GLONASS
3. All satellites are GPS satellites
4. All satellites are GLONASS satellites

The GPS and GLONASS standard deviations are assumed to equal  $\sigma_{PR_{GPS}} = 30\text{m}$  and  $\sigma_{PR_{GLONASS}} = 15\text{m}$ .

Despite the simplicity of the example, we can draw two important conclusions:

- The same measurement configuration with the same integrity leads to different iDOP values and identical BIT values due to the different scalings
- An improvement of the measurements by a factor 2 leaves the iDOP unchanged, but improves the BIT by a factor 4

We will see in the next section, that the improvement of a factor 4 is really related to an improvement in integrity of a factor 4 (this will simply follow from the definition of the BIT). In other words: the BIT that we will define in the next section does not have the disadvantages from the iDOP, and its value is an absolute measure of integrity.

<sup>2</sup> An extra problem with the ARP is, that it is based on the approximate relation (5.5) between position bias and test statistic, that will become less valid when more noise is present.

## 7. The Bias Integrity Threat

Because integrity not only depends on measurement geometry, but also on the amount of measurement noise, we will introduce a new integrity metric (BIT), that takes both influences into account. In section 8, we will further generalize its definition to the multiple failure scenario.

Lets assume that the variance of all measurements is the same ( $R_v = \sigma^2 I$ ). When the unknowns that have to be determined are the position  $[x \ y \ z]$  and the clock bias  $b$ , they have a covariance (3.5)

$$R_{\hat{x}} = \sigma^2 (H^T H)^{-1} \quad (7.1)$$

The sum of the variances of the unknown parameters can therefore be written in terms of measurement quality ( $\sigma$ ) and geometry (DOP, see (4.2)) as:

$$\sigma_x^2 + \sigma_y^2 + \sigma_z^2 + \sigma_b^2 = \text{trace}(R_{\hat{x}}) = \sigma^2 \cdot DOP^2 \quad (7.2)$$

As follows straightforwardly from (4.1), the worst drop in precision caused by removing a satellite can be factored in exactly the same way in a signal quality ( $\sigma$ ) and a geometric (iDOP) part:

$$\text{max. drop in trace}(R_{\hat{x}}) = \sigma^2 \cdot iDOP \quad (7.3)$$

We can conclude that an increase of the noise variance will worsen both position accuracy and system integrity, although the values of DOP and iDOP remain the same. As (7.3) already suggests, the integrity is much better described by the product of the iDOP and the measurement variance. This means that we can define a new integrity metric, the Bias Integrity Threat<sup>3</sup>, as:

$$BIT = \sigma^2 \cdot iDOP \quad (7.4)$$

As we can see from (5.1) the following equivalence holds when  $R_v = \sigma^2 I$ :

$$\begin{aligned} \sigma^2 \cdot iDOP &= \max_i \frac{\| (H^T H)^{-1} H^T \tilde{\mu}_v^{(i)} \|^2}{\| (I - H(H^T H)^{-1} H^T) \tilde{\mu}_v^{(i)} \|^2_{\frac{1}{\sigma^2} I}} \\ &= \max_i \frac{\| \Delta \hat{x}_{LS}(\tilde{\mu}_v^{(i)}) \|^2}{\lambda(\tilde{\mu}_v^{(i)})} \end{aligned} \quad (7.5)$$

<sup>3</sup> In [Ober96], we use the term 'GiDOP' (Generalized integrity DOP) instead of BIT. Because it represents more than just integrity geometry, we decided that BIT is more appropriate.

in which we recognize the noncentrality parameter of the test statistic (3.14) in the denominator. The ratio of (7.5) indicates to what extent biases can cause unacceptable position errors without being detectable, which justifies why we have called it the Bias Integrity Threat. Note that the norm of the influence of a bias on the test statistic is weighted by the inverse noise covariance: *it is exactly this weight matrix that incorporates the decreased bias detectability for increased noise levels in the BIT.*

We can easily generalize the definition of the BIT from (7.4) to measurements with different standard deviations. We simply drop the constraint  $R_v = \sigma^2 I$  and compute the position bias and the noncentrality parameter in (7.5) by using weighted least squares, giving:

$$\begin{aligned} BIT &= \max_i \frac{\| \Delta \hat{x}_{LS}(\tilde{\mu}_v^{(i)}) \|^2}{\lambda(\tilde{\mu}_v^{(i)})} = \max_i \frac{\| N \tilde{\mu}_v^{(i)} \|^2}{\| D \tilde{\mu}_v^{(i)} \|_{R_v^{-1}}^2} \\ &= \max_i \frac{\tilde{\mu}_v^{(i)T} N^T N \tilde{\mu}_v^{(i)}}{\tilde{\mu}_v^{(i)T} D^T R_v^{-1} D \tilde{\mu}_v^{(i)}} \end{aligned} \quad (7.6)$$

Due to the different weights that are attached to the measurements, it will no longer be possible to determine the contributions of geometry and measurement quality in (7.6) separately.

## 8. Integrity and the more failure assumption

The handling of the situation in which multiple measurements are assumed to be possibly failing is slightly more difficult than the single failure case. A very important observation is, that failing measurements can still be used to check their mutual correctness! This makes it too conservative to look at the drop in accuracy that would be caused by removing multiple satellites from the position solution, as is proven in [Ober96].

When  $r$  failures occur simultaneously, the bias vectors that we try to detect will have  $r$  nonzero elements. As soon as  $r > 1$ , the exact direction of the bias vector becomes important. We will use a worst case approach again, and look at the worst direction of all bias vectors with  $r$  nonzero elements.

To find this worst case direction, we will exploit a standard result from linear algebra. For two positive definite  $r \times r$  matrices  $X^T X$  and  $Y^T Y$ , the maximum of the so-called Rayleigh's quotient over all  $r$ -vectors  $\tilde{\mu}_r$  equals the largest eigenvalue of  $(Y^T Y)^{-1} X^T X$  [Strang86]:

$$\max_{\tilde{\mu}_r} \frac{\tilde{\mu}_r^T X^T X \tilde{\mu}_r}{\tilde{\mu}_r^T Y^T Y \tilde{\mu}_r} = \lambda_{\max} \left( (Y^T Y)^{-1} X^T X \right) \quad (8.1)$$

We have to realize that the matrices in the denominator of (7.6) are only positive semi-definite. This implies that if we allow too many measurements to become biased, the maximum BIT will become infinite as some biases will become completely invisible. When we allow at most  $n-m$  measurements to be unbiased, we can use the previous result when we select appropriate full rank, positive definite submatrices. We can do this by removing the parts that correspond to zeros in the assumed bias vector. The BIT can then be written as:

$$BIT = \max_{\tilde{\mu}_v^{(i)}} \frac{\tilde{\mu}_v^{(i)T} N^T N \tilde{\mu}_v^{(i)}}{\tilde{\mu}_v^{(i)T} D^T R_v^{-1} D \tilde{\mu}_v^{(i)}} = \max_i \left\{ \lambda_{\max} \left( Q^{(i)} \right) \right\} \quad (8.2)$$

in which the  $r \times r$  'quotient matrix' is

$$Q^{(i)} = \left( \tilde{D}^{(i)T} R_v^{-1} \tilde{D}^{(i)} \right)^{-1} \tilde{N}^{(i)T} \tilde{N}^{(i)} \quad (8.3)$$

In this equation,  $\tilde{N}^{(i)}$  and  $\tilde{D}^{(i)}$  are the matrices that are obtained when we remove all columns that correspond to zero elements in  $\tilde{\mu}_v^{(i)}$  from  $N$  and  $D$  respectively.

The reader is referred to the appendix for a computational example that might clarify the equations in this section. It also shows how we can interpret the BIT in geometrical terms when all measurements have the same variance.

A last remark on the computation of (8.2): when the number of unknowns of interest  $m$  is smaller than the number of assumed biases  $r$ , it is computationally more attractive to use the following  $m \times m$  quotient representation  $Q^{(i)}$  instead of  $Q^{(i)}$  that is  $r \times r$ :

$$Q^{(i)} = \tilde{N}^{(i)} \left( \tilde{D}^{(i)T} R_v^{-1} \tilde{D}^{(i)} \right)^{-1} \tilde{N}^{(i)T} \quad (8.4)$$

This matrix has the same maximum eigenvalue as  $Q^{(i)}$ , but the corresponding eigenvector is no longer the bias vector for which (8.2) reaches its maximum.

## 9. The Maximum Undetectable Position Bias

The appendix shows an example in which the ratios from (7.6) and (8.2) are computed for different biases. Figure 4 shows how the BIT can be interpreted as the slope of the square position error plotted against the noncentrality parameter of the distribution of the test statistic. We can therefore find the Maximum Undetectable Position Bias (MUPB) as

$$MUPB = \sqrt{BIT \cdot \lambda_{\min}} \quad (9.1)$$

in which  $\lambda_{\min}$  is the smallest value of the noncentrality parameter that can be detected with sufficient probability.

The MUPB could be used as an alternative integrity metric instead of the BIT. It uses a similar approach as the ARP does: they both relate the test statistic to a maximum position bias. But instead of using the *approximate* relation between the position bias and the noisy test statistic itself (5.4), the MUPB exploits its *exact* relation with the noncentrality parameter of the test statistic's distribution. The logic of this should be clear: as we have seen from (3.16), it is precisely the noncentrality parameter that determines the amount of detection power!

## 10. Integrity and Kalman filtering

In this section we will indicate how it is possible to use the BIT and MUPB in a Kalman filter environment. The integrity of Kalman filters is often questioned [Michalson95]. We will show that this might not be necessary, because the worst case effects of biases in the Kalman filter can be determined by the integrity metrics that we have developed. The approach is simple: we write the Kalman filter measurement update in the form of a regression model, to which the BIT and MUPB can be applied. Due to the recursive character of Kalman filter based position computation, special care should be taken in the assumption on the biases that can be present.

The Kalman filter computes a predicted position  $\hat{x}^-$  and a corresponding covariance matrix  $R_{\hat{x}^-}$ , based on the last position and a dynamic model  $\Phi$  that relates the past position to the current one:

$$\hat{x}_{k+1}^- = \Phi \hat{x}_k^- + \bar{w}_{k+1} \quad (10.1)$$

in which  $\bar{w}$  is white, Gaussian noise, and the index  $k$  indicates time. The total noise on this prediction is the sum of the noise in the dynamic model  $\bar{w}$ , and the noise on the previous position estimation. We will use the notation  $\bar{w}'$  for this prediction noise:

$$w'_{k+1} = \Phi_k (\bar{x}_k - \hat{x}_k) + \bar{w}_{k+1} \quad (10.2)$$

and denote its covariance by  $R_w$ . The prediction is used in the same way as all other measurements. The measurement update of the Kalman filter determines a new position estimate by computing a weighted least squares solution of the following equation [Kovacevic92]:

$$\begin{bmatrix} \hat{x}_{k+1}^- \\ \bar{z}_{k+1} \end{bmatrix} = \begin{bmatrix} I \\ H_{k+1} \end{bmatrix} \bar{x}_{k+1} + \bar{\varepsilon}_{k+1} \quad (10.3)$$

This is a linear regression model in which the noise and its covariance are defined as:

$$\bar{\varepsilon}_{k+1} = \begin{bmatrix} w'_{k+1} \\ \bar{v}_{k+1} \end{bmatrix} \quad (10.4)$$

$$R_{\varepsilon_{k+1}} = \begin{bmatrix} R_w & 0 \\ 0 & R_v \end{bmatrix} \quad (10.5)$$

Now that we have written the Kalman filter in the form of a regression model, we can use the earlier obtained results to determine a metric for the 'worst case' integrity. The only thing that is important to realize is that, once a bias occurred, it will effect the position estimation, and therefore the prediction of the next position as well. In other words, measurement biases are propagated in time by the dynamic model, which can be dangerous if not taken into account. It is possible to compute exactly how undetected measurement biases get propagated, see for some approaches [Salzmann93] and [Willsky76]. However, these methods generally neglect the possibility that biases in the measurements and the dynamic model occur simultaneously.

A conservative, worst case approach that could be taken is to assume that the entire position prediction might be biased. This means that we assume that biases of the following form might occur in the model (10.3):

$$\bar{\mu}_{\varepsilon}^{(i)} = [\mu_1 \cdots \mu_m \ 0 \cdots 0 \ \mu_i \ 0 \cdots 0]^T \quad (10.6)$$

in which the first  $m$  biases correspond to the position prediction. It can be proven [Ober96] that this approach always gives higher BIT values for the Kalman filter than for the regression model. This is not surprising, because we assume that all extra added measurements might be in error, and we use a worst case approach.

*However, the guaranteed position precision that a Kalman filter offers might still be better than that of the regression model! This can be seen as follows (see also figure 3). The position precision that RAIM/AAIM can*

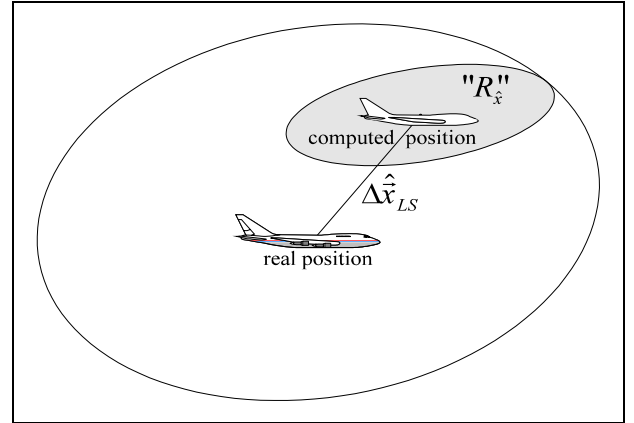


**Figure 3. The bound on the position error that is guaranteed by RAIM/AAIM**

warrant is the sum of the Maximum Undetectable Position Bias (caused by a nonzero mean of the noise) and the position uncertainty (caused by the covariance of the noise). The increased precision that the Kalman filter provides might very well compensate for the larger position bias that can be protected against!

Preliminary computations at Delft University indicate that the Maximum Undetectable Position Bias of the Kalman filter is only slightly smaller than the one of the regression model, when the assumed noise covariance of the dynamic model is not taken too small. More research will be necessary to give a definite answer to the question whether the Kalman filter outperforms the regression model in terms of guaranteed position precision or not.

## 11. Concluding remarks

We have introduced two new metrics for RAIM/AAIM integrity monitoring, that can be used in multiple failure scenarios and with general measurement covariance matrices (of which the Kalman filter is a special case). The BIT and the MUPB go beyond geometric considerations alone, and takes signal quality into account as well. Their values are absolute integrity metrics rather than relative ones such as the  $\delta H_{\max}$  (iDOP) or the ARP, and are therefore easy to interpret. Even in the case of multiple failures, their computation only requires the determination of the largest eigenvalue of a small matrix, which makes them well suitable for use in real time applications. The BIT and the MUPB provide insight in the minimum integrity performance of Kalman filters, and can become a useful tool in answering the question whether it is safe and/or profitable to use a Kalman filter instead of a regression model.

## ACKNOWLEDGMENT



The author would like to thank ir. D.J. Moelker for his help in the preparation of this paper.

## REFERENCES

- [Brown90]Brown, A.K. and M.A. Sturza; "The effect of geometry on Integrity Monitoring Performance", proceedings of the ION annual meeting, June 1990
- [Brown92b]Brown, R.G.; "A Baseline RAIM scheme and a Note on the equivalence of three RAIM Methods", ION, 1992, pp 127-137
- [Brown96]Brown, R.G.; "Receiver Autonomous Integrity Monitoring", in "*Global Positioning System: theory and applications Volume 2*", eds. B.W. Parkinson and J.J. Spilker Jr., American Institute of Aeronautics and Astronautics, 1996
- [Kovacevic92]Kovacevic B.D., Z.M. Durovic and S. Glavaski; "On robust Kalman filtering", Int. J. Control, Vol. 56, No. 3, pp. 547-562, 1992
- [Michalson95]W.R. Michalson; "Ensuring GPS Navigation integrity using Receiver Autonomous Integrity Monitoring", IEEE AES Systems Magazine, pp. 31-34, October 1995
- [Ober96] Ober, P.B.; "Integrity Monitoring: information paper", TVS memorandum REP9606B, Delft University of Technology, Faculty of Electrotechnics, TVS Group, June 1996
- [Rao95] Rao, C.R. and H. Toutenburg; "Linear Models: least squares and alternatives", Springer, 1995
- [Salzmann93] Salzmann, M.A.; "Least Squares Filtering and Testing for Geodetic Navigation Applications", Ph.D. Dissertation, Delft University of Technology, 1993
- [Strang86] Strang, G; "Linear Algebra and its applications", 3<sup>d</sup> edition, Harcourt Brace Jovanovich Publishers, San Diego, 1986
- [Sturza90] Sturza, M.A. and A.K. Brown; "Comparison of fixed and variable threshold RAIM algorithms", proceedings of ION, pp. 437-443, 1990
- [Willsky76]Willsky, A.S.; "A survey of design methods for failure detection in dynamic systems", Automatica, Vol. 12, pp. 601-611, 1976

## Appendix: An example

To show how to compute the BIT for multiple failures, we will provide a simple example. We navigate in a two dimensional plane, and assume no clock bias is present. There are four satellites at angles 35°, 100°, 190° and 235°. For simplicity, all measurements have the same standard deviation 1, which will allow us to give a simple geometrical interpretation for the worst case bias. Figure 5 shows the satellite positions, the measurement biases and the position error for this worst case.

The observation matrix from (2.1) is given by:

$$H = \begin{bmatrix} -\cos(35^\circ) & -\sin(35^\circ) \\ -\cos(100^\circ) & -\sin(100^\circ) \\ -\cos(190^\circ) & -\sin(190^\circ) \\ -\cos(235^\circ) & -\sin(235^\circ) \end{bmatrix} \quad (A-1)$$

which gives the following matrices that relate the measurement bias to the position error (3.6) and mean noise estimation (3.7) respectively:

$$N = \begin{bmatrix} -0.3527 & 0.4083 & 0.5795 & 0.1211 \\ -0.1211 & -0.6842 & -0.1855 & 0.3527 \end{bmatrix} \quad (A-2)$$

$$D = \begin{bmatrix} 0.6416 & -0.0580 & 0.3684 & 0.3015 \\ -0.0580 & 0.2552 & -0.2833 & 0.3263 \\ 0.3684 & -0.2833 & 0.4615 & -0.1805 \\ 0.3015 & 0.3263 & -0.1805 & 0.6416 \end{bmatrix} \quad (A-3)$$

We assume that at most 2 measurements can be biased simultaneously. Table 2 shows the worst case "BIT-ratios"

$$\frac{\bar{\mu}_v^{(i)T} N^T N \bar{\mu}_v^{(i)}}{\bar{\mu}_v^{(i)T} D^T D \bar{\mu}_v^{(i)}} \quad (A-4)$$

for all combinations of 1 or 2 erroneous satellites. The overall worst case is the one in which satellite 2 and 3 are biased. We will show the computation of (A-4) for this pair of satellites. Figure 4 shows how the values of the BIT-ratio can be interpreted as the slope in the plot of the square position error against the noncentrality of the distribution of the test statistic. The Maximum Undetectable Position Bias (MUPB) follows straightforwardly from (9.1).

The bias has the form

$$\bar{\mu}_v^{(2,3)} = [0 \ \mu_2 \ \mu_3 \ 0]^T \quad (A-5)$$

in which the individual sizes of the bias on satellite 2 ( $\mu_2$ ) and 3 ( $\mu_3$ ) are still unknown. We will compute worst case values for them now.

When we select the correct columns from  $N$  and  $D$  we become the submatrices from (8.3):

$$\tilde{N}^{(2,3)} = \begin{bmatrix} 0.4083 & 0.5795 \\ -0.6842 & -0.1855 \end{bmatrix} \quad (A-6)$$

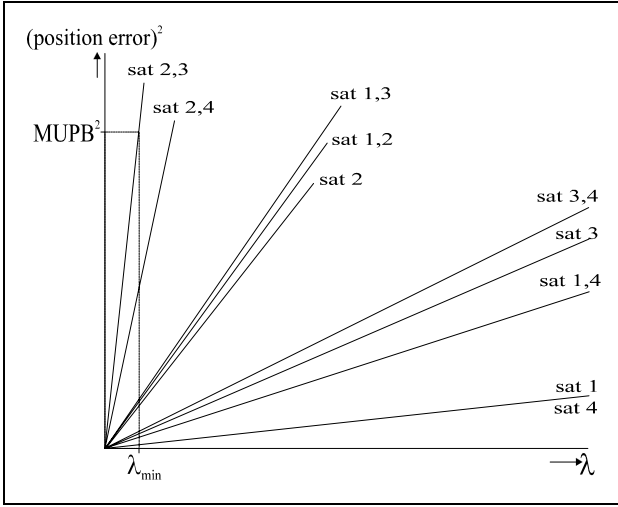


Figure 4. The BIT for different biases

$$\tilde{D}^{(2,3)} = \begin{bmatrix} -0.0580 & 0.3684 \\ 0.2552 & -0.2833 \\ -0.2833 & 0.4615 \\ 0.3263 & -0.1805 \end{bmatrix} \quad (\text{A-7})$$

and the quotient matrix (8.3) becomes

$$Q^{(2,3)} = \begin{bmatrix} 10.5514 & 7.2653 \\ 7.2653 & 5.2626 \end{bmatrix} \quad (\text{A-8})$$

This matrix has the following eigenvalues and corresponding eigenvectors:

$$\lambda_1 = 0.1745, \quad \vec{v}_1 = [0.5736 \quad -0.8192]^T \quad (\text{A-9})$$

$$\lambda_2 = 15.6386, \quad \vec{v}_2 = [0.8192 \quad 0.5736]^T \quad (\text{A-10})$$

The maximum eigenvalue equals 15.6386, which indicates that when the smallest bias we can detect with enough probability has a size of 1 meter, the corresponding (maximum) position error equals  $\sqrt{15.6386}$  meter. This maximum position error is reached when the biasvector lies in the direction given by the largest eigenvector  $\vec{v}_2$  extended with zeros in the nonbiased directions:

$$\vec{\mu}_v^{(2,3)} = \|\vec{\mu}_v^{(2,3)}\| \cdot [0 \quad 0.8192 \quad 0.5736 \quad 0]^T \quad (\text{A-11})$$

This is exactly the bias that causes a position error perpendicular to the line that connects the two errorfree satellites (3.6):

$$\Delta \hat{x}_{LS} = \|\Delta \hat{x}_{LS}\| \cdot [0.7071 \quad -0.7071]^T \quad (\text{A-12})$$

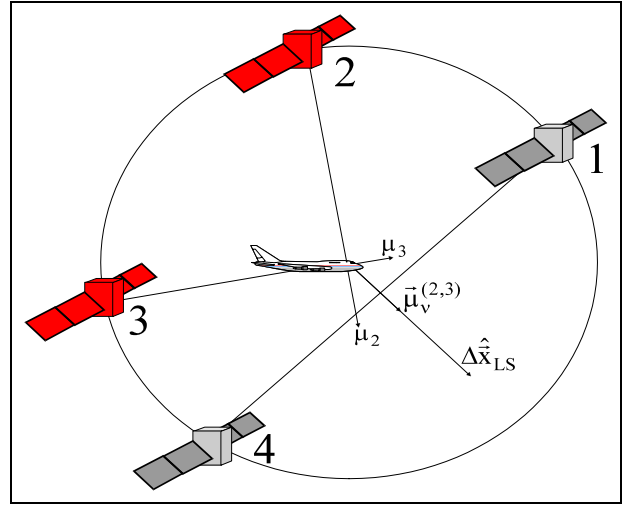


Figure 5. The worst case influence of multiple failures and its relation to satellite geometry

Because the two erroneous satellites are placed at a mutual angle of  $90^\circ$ , they can not be used to checked each other. This means that the other two satellites have to provide the entire redundancy, that is weakest in the direction that is perpendicular to the line between them.

biased satellite(s)	BIT-ratio
sat 1	0.2167
sat 2	2.4875
sat 3	0.8024
sat 4	0.2167
sat 1 + sat 2	2.5064
sat 1 + sat 3	2.6738
sat 1 + sat 4	0.6598
sat 2 + sat 3	15.6386
sat 2 + sat 4	10.8231
sat 3 + sat 4	0.9449

Table 2. BIT-ratios for different biases